A Unifying Hypothesis for both Pendular and Jerk Waveforms in Infantile Nystagmus Embodied in a Behavioral Ocular Motor System Model

Zhong WANG[1,3], Louis F. DELL'OSSO[1-3], and Jonathan B. JACOBS[1,2]

[1] The Daroff-Dell'Osso Ocular Motility Laboratory, Louis Stokes Cleveland Department of Veterans Affairs Medical Center and CASE Medical School, Cleveland, OH, USA
[2] Dept of Neurology, Case Western Reserve University and University Hospitals of Cleveland, Cleveland, OH, USA
[3] Dept of Biomedical Engineering, Case Western Reserve University, Cleveland, OH, USA

ABSTRACT

The original behavioral Ocular Motor System (OMS) model for Infantile Nystagmus Syndrome (INS) simulated the responses of individuals with several pendular (P) waveforms based on a hypothesized exacerbation of the normal pursuit-subsystem instability and its interaction with other OMS components. The simulation of jerk (J) waveforms and the easy transition between J and P waveforms were not included in that model. To expand this behavioral model, we intend to incorporate J waveforms with a unifying mechanism for both types of INS waveforms. The transition from a P to a J waveform required that braking saccades become foveating saccades. That simple change produced an alternating-direction J waveform. To convert it into a unidirectional-jerk waveform, the underlying pendular oscillation frequency of the model was varied and the oscillation reset with each foveating saccade. The result was a unidirectional J waveform. The use of a resettable neural integrator in the pursuit pre-motor circuitry enabled the resetting. Other functional blocks within the OMS model were also modified. The fixation subsystem remained responsible for elongating foveation periods in J and P waveforms. The simulations of this robust behavioral OMS model demonstrate that both P and J waveforms can be generated by the *same* pursuit-system instability; this supports the hypothesis that most INS waveforms are due to a loss of pursuit-system damping. Modeling OMS dysfunction continues to provide valuable insight into the functional structure of the OMS under both normal and pathological conditions.

Keywords: Infantile Nystagmus, Ocular Motor System, Eye Movements, Model

1. INTRODUCTION

Nystagmus, the rhythmic to-and-fro oscillation of the eyes, has been regarded as enigmatic since ancient times. The word "nystagmus" comes from the Greek word, νυσταγμός (drowsiness); it is derived from νυστάζειν, meaning, "to nod in one's sleep." These involuntary movements of the eyes could be one of several infantile types or may be acquired later in life. Infantile Nystagmus Syndrome (INS) [1] may exhibit either pendular or jerk waveforms, and the slow phases are increasing velocity (or "runaway") exponentials, though approximately linear slow phases account for some less-common waveforms, such as triangular, bidirectional jerk, and some pure jerk [2,3]. INS frequently accompanies additional afferent defects of the visual sensory system such as albinism, achromatopsia, congenital cataracts, optic nerve and/or foveal hypoplasia. When it occurs without other sensory deficits, INS may still reduce visual acuity to a variable extent, depending on the foveation characteristics of the nystagmus waveform. INS is predominantly horizontal, with some torsional and, rarely, vertical motion. Despite the oscillation, individuals with INS experience no oscillopsia [4,5]. The *primary subsystem instability* in IN is hypothesized to lie in the normally underdamped smooth pursuit system; vestibular dysfunction (imbalance) may also be present. Less often, the nucleus of the optic tract may be involved [5,6].

It is not until the past few decades that technologic advances permitted quantitative insights into the complexity of nystagmus waveforms and the ocular motor system. Along with the understanding of nystagmus came a variety of surgical procedures that could help nystagmus patients improve their impaired vision [7]. Top-down, behavioral models were also built which are capable of simulating human ocular motor responses to known target inputs in the presence of nystagmus and saccadic disorders [8-11]. The basis for many of these attempts was accurate recording of eye movement responses to visual stimuli under properly designed recording paradigms. Accurate data calibration and analysis (leading to evaluation of potential visual acuity) are also essential in exploiting possible conditions that could damp the nystagmus and suggesting therapies accordingly [12-14].

The concept of our ocular motor system (OMS) model arose from our realization that complex biological control systems cannot be accurately or usefully simulated on a piecemeal basis consisting of small, independent subsystems. Since there are an infinite number of solutions to simulating specific waveforms, models that merely generate waveforms that resemble IN in isolation are of little use, either clinically or to increase our understanding of the underlying mechanisms of IN. A biologically relevant model of the INS should be part of, and operate within, a complete OMS model, capable of reproducing the normal ocular motor *behavior* of these individuals while still oscillating. Our OMS model evolved from models that were built on years of observation and analysis of normal and abnormal eye movement data; wherever applicable, adherence to demonstrated neurophysiological structure was maintained. This model adopts a top-down, engineering-based approach—no speculations are made on possible anatomical sites for each functional block (e.g., fixation and the superior colliculus) or on the putative roles of specific neurons (e.g., omnipause and burst cells). Emphasis is put on how each functioning block communicates with each other in this complex system and how subsystems work together under organizing principles to exhibit "real" ocular motor system behaviors. This approach helped ensure that the model would be "robust" in its behavior, meaning that: 1) it would respond realistically to a broad range of inputs, simulating a broad range of behaviors; and 2) in the

more classical control-systems definition of the term, it would recover from internal errors in a realistic manner, rather than simply failing or yielding uncontrolled outputs [10].

The OMS model for INS simulated the responses of individuals with several pendular waveforms, e.g. Pfs (pendular with foveating saccades, and PPfs (pseudopendular with foveating saccades). It was based on a hypothesized exacerbation of the normal pursuit-subsystem instability and its interaction with other OMS components. The OMS model consists of smooth pursuit (SP) and saccadic subsystems, and an "Internal Monitor" (IM) that receives afferent information from the retina plus position and velocity efference copy to determine the control signals that drive these motor subsystems (Figure 1). The OMS model uses efference copy to reconstruct target position and velocity; these are the signals that drive the saccadic and pursuit systems, respectively. The model contains only functional blocks known to be part of the OMS. Accurate model simulations during fixation, saccades to known targets (steps, pulses, and pulse-steps), and smooth pursuit (ramps and step-ramps), as well as many emergent properties and unexpected predictions of the model duplicated the recorded responses of humans with INS—providing strong support for the hypothetical mechanisms contained within the model [9,10].

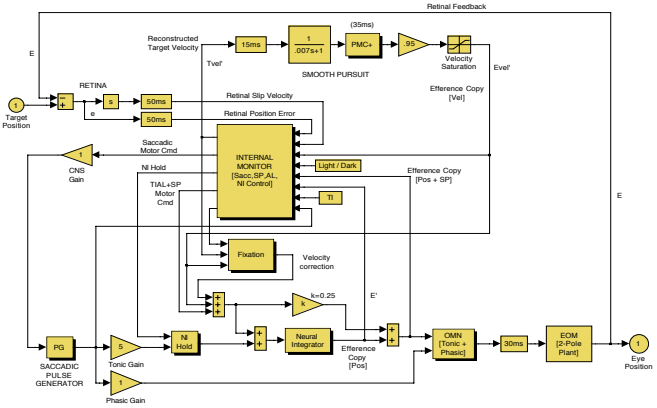

Figure 1. Block diagram of behavioral OMS model with smooth pursuit subsystem shown. PMC+ = Pre-Motor Circuitry; Sacc = Saccade; SP = Smooth Pursuit; AL = Alexander's Law; TI = Tonic Imbalance; PG = Pulse Generator; NI = Neural Integrator; OMN = Ocular Motor Neuron; EOM = ExtraOcular Muscle.

There are a number of features of INS that were not included in the original OMS model; one is the simulation of jerk waveforms. To expand this behavioral model, we intend to demonstrate that jerk waveforms may originate from a unifying mechanism producing both pendular and jerk waveforms.

2. METHODS

Recording

The ocular motor recordings and observations used for the computer simulation came from approximately 1000 subjects with INS, who were recorded in our laboratory over the past 35 years. Written consent was obtained from subjects before the testing. Subjects were seated in a chair with headrest and chin stabilizer, far enough from an arc of red LEDs to prevent convergence effects (>5 feet). At this distance the LED subtended less than 0.1° of visual angle. The room light could be adjusted from dim down to blackout to minimize extraneous visual stimuli. Experiments usually consisted of from one to ten trials, each lasting under a minute with time allowed between trials for the subject to rest. Trials were kept this short to guard against boredom because INS intensity is known to decrease with inattention.

Eye movements were measured using either an infrared reflection (IR, eye-trac 210, ASL, Waltham, MA), a magnetic scleral search coil (C-N-C Engineering, Seattle, WA), or a high-speed digital video (EyeLink II, SR Research, Mississauga, ON, Canada) system. The IR system was linear to ±20° in the horizontal plane and monotonic to 25-30° with a sensitivity of 0.25°. The search-coil system had a linear range greater than ±20°, a sensitivity of 0.1°, and crosstalk less than 2.5%. Each coil was pre-calibrated using a protractor device. The digital video system had a linear range of ±30° horizontally and ±20°vertically. System sampling frequency was 500 Hz, gaze position accuracy error was 0.5°-1° on average, and pupil size resolution was 0.1% (0.02 mm change in diameter reliably detectable). The total system bandwidth for all systems (position and velocity) was 0-100 Hz. The data from all systems were digitized at 500 Hz with 16-bit resolution.

The position signal for each eye was adjusted with the other eye behind cover to obtain accurate position information; the foveation periods were used for zero-adjustment (all systems) and calibration (IR or video). Eye positions and velocities (obtained by analog differentiation of the position channels) were displayed on a strip chart recording system. Monocular primary-position adjustments for all methods allowed accurate position information and documentation of small tropias and phorias hidden by the nystagmus.

Analysis

All the analysis and graphics were done in MATLAB environment (The MathWorks, Natick, MA) using the OMtools software available on http://www.omlab.org ("Software and OMS Models" page). Only eye position was sampled directly; velocity was derived from the position data by a 4th order central-point differentiator; acceleration was derived from the velocity data by the same differentiator. Position data were pre-filtered with a low-pass filter with the cutoff frequency of 50 Hz to get rid of the noise without changing the nystagmus signals to be studied. Only data from the fixating eyes were analyzed.

Simulation

All ocular motor simulations were performed in MATLAB Simulink (Waltham, MA) environment.

3. RESULTS

We used the same "evolutionary" procedure to generate jerk waveforms as had been employed for pendular waveforms. To change the system's underlying pendular oscillation, the saccadic subsystem had to be modified to correctly perform under those conditions when foveating saccades should be generated. The transition from PPfs waveform to a jerk waveform required that braking saccades be replaced by foveating saccades. The saccadic subsystem consists of a pulse generator, IM, and the same neural integrator, ocular motor neuron, and two-pole plant used in the SP subsystem. We first altered the functional block ("Breaking/Foveating Saccade Logic") within the IM. This block contains the logic that would normally trigger the braking saccades of IN or fast phases of induced nystagmus (e.g., vestibular or optokinetic). A simple

modification to this functional block gave rise to alternating-direction jerk nystagmus (i.e., whose foveating saccades were made in alternating directions from both sides of the target). Figure 2 shows an interval of fixation at primary position that simulates an individual with INS who exhibited an alternating-direction jerk nystagmus.

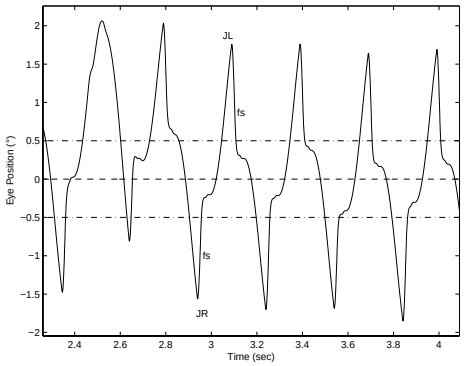

Figure 2. Alternating-direction jerk nystagmus. Fixation data at primary position are shown. In this and subsequent Figures, dashed lines indicate target position, dash-dotted lines around target-position indicate foveal extent (±0.5°), JR = jerk right, JL = jerk left, and fs = foveating saccade.

To convert an alternating-direction jerk waveform into a unidirectional-jerk waveform, several other modifications were necessary. First of all, the underlying pendular oscillation frequency of the model needed to be lowered. The pre-motor circuitry (PMC+) had its oscillation frequency at ~3.5 Hz, based on parameters from the altered Robinson model [10,15]. If those waveforms were to be "split" into a unidirectional jerk, the frequency would be ~7 Hz. This frequency was above average for most individuals with jerk INS waveforms. To lower the oscillation frequency, we changed the delay in the feedback loop of PMC+ to be 40 ms, which was twice the original value. This yielded the oscillation frequency of ~2.5 Hz which results in a unidirectional jerk nystagmus of ~5 Hz.

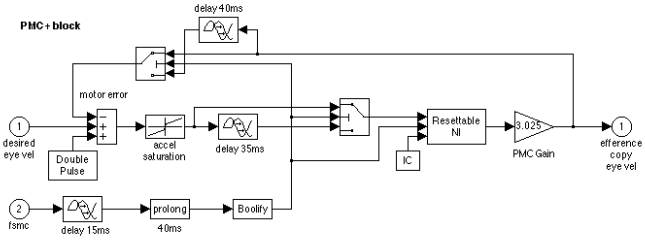

Figure 3. Modified premotor circuitry (PMC+) block in the OMS model. The PMC+ block generates a restarted oscillation for every jerk nystagmus cycle, using resetting signals (delayed, prolonged and boolified) from foveating saccade motor command.

Secondly, the oscillation needed to be reset when each foveating saccade was made. The use of a resettable neural integrator in PMC+ accomplished the resetting (Figure 3). This neural integrator has the same structure as the one in pulse generator [16-18], distinct from the common neural integrator that appears in the final motor pathway. We used the motor command for foveating saccades as a resetting signal, i.e., when the BS/FS logic box indicated the need to generate a foveating saccade, the pendular oscillation underlying pendular waveforms was reset. The foveating-saccade motor command was appropriately prolonged (40 ms) and delayed (15 ms). Due to the time delays in both the feedback and feedforward loops, the resetting required that those time delays also be reset (i.e., the stored energy was dumped).

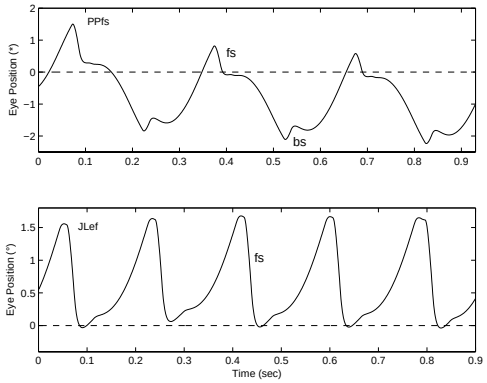

Figure 4. Comparison of foveating saccade and braking saccade in PPfs and jerk waveforms. Fixation data at primary position are shown. PPfs = PseudoPendular with foveating saccades, JLef = Jerk Left with extended foveation, and bs = braking saccade.

Thirdly, the BS/FS logic was further modified to accurately generate foveating saccades in jerk waveforms. Those saccades are different from the foveating and braking saccades in the PPfs waveforms (Figure 4). Braking saccades are automatically generated to brake runaway eye velocities. For the PPfs waveform, the logic necessary to decide whether a saccade will be braking or foveating is the following: If the eye is running away from the target at the time of saccade programming (which precedes the actual time the saccade is generated), the velocity exceeds a user-settable threshold (default = 4°/s), and has passed its point of maximum velocity (i.e., is not still accelerating), a braking saccade will be generated. This is consistent with the definition of a braking saccade [19,20]. If, however, the eye is approaching the target at that time, and the velocity exceeds the threshold, and falls below the acceleration threshold, then the saccade will be foveating, with the magnitude and direction calculated by the predicting where the eye will be 60 ms later (default value based on the current distribution of internal delays in the model), when the saccade will occur. In jerk waveforms, foveating saccades are made when the eye is running away from target, just as braking saccades are. Under this circumstance, the logic for foveating saccade timing was the same as for braking saccades in the PPfs case. However, there are distinct differences between the amplitude of those two types of saccades. Braking saccades have small, stereotyped amplitudes independent of the eye's position vis-à-vis the target, while the foveating saccades we wish to generate for jerk waveforms are larger and must accurately correct the position error. The magnitude was calculated by predicting where the eye would be 60 ms later (when the saccade would occur), similar to the method for calculating the amplitudes of foveating saccades in PPfs.

The modifications described above resulted in a unidirectional jerk waveform. The fixation subsystem remained responsible for elongating the low-velocity intervals of foveation in jerk waveforms, as it did in Pfs and PPfs waveforms: as a result, the

jerk waveform simulated was jerk with extended foveation (Jef). Figure 5 shows simulations of the model responding to different visual inputs. Both jerk right and jerk left waveforms consistently returned to the target after foveating saccades were generated; although there were slight differences between the sizes of each saccade, final target-image position always remained within the ± 0.5° foveal area (which allows the best visual acuity). The model also responded well to step changes in target position with different directions, latencies and durations. However, it took a greater than normal amount of time for the eye to arrive on target (the time varied from 2 to 3 cycles, i.e., ~400 to 600 ms).

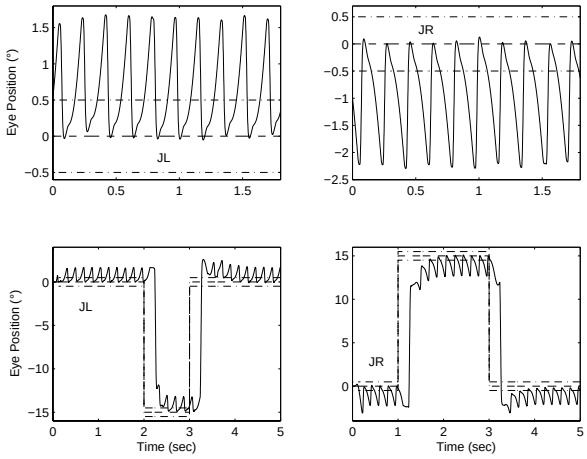

Figure 5. OMS model responses at primary position and for 15° step inputs. Upper panels show fixation data for jerk left and jerk right waveforms, respectively; lower panels show model responses to step inputs with different directions, onset times and durations.

The model outputs and human data showed great similarity, as demonstrated in Figure 6. Due to idiosyncratic differences in INS waveforms, the human data showed a larger cycle-to-cycle variance; some of the "foveation periods" were out of the fovea, indicating lowered visual acuity.

4. DISCUSSION

When the OMS model was completed in 2003, it simulated the most complex INS waveforms (Pfs, PPfs) consistent with INS data. It demonstrated that our hypothesis for the generation of P, Pfs, and PPfs could be realized by a functionally normal OMS without diminishing the responses to a broad variety of target stimuli. Although jerk INS is the simplest waveform to simulate using any of several methods, we did not hypothesize about its mechanism at that time because of the need to allow easy transitions with pendular waveforms when gaze is shifted. We did not add a separate mechanism for jerk waveforms to the current version of the OMS model because we believe that, in agreement with observations and accurate eye movement recordings on inattention and waveform transition, the pendular and jerk waveforms are derived from the same underlying mechanism, i.e., an undamped smooth pursuit subsystem.

Most INS patients exhibit both pendular and jerk waveforms and easily change from one to the other as gaze angle is changed. Figure 7 illustrates a nystagmus waveform transition between PPfs and Jef in an individual with INS fixating a target at -5°. The gaze angle at which this transition happens is idiosyncratic, depending on the null position and sharpness.

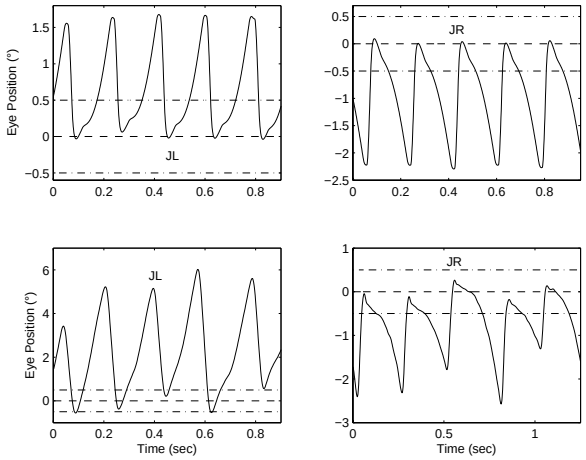

Figure 6. Comparison of simulated jerk waveforms and human data. Upper panels show simulations from the OMS model; lower panels show human data. Fixation data at primary position is shown.

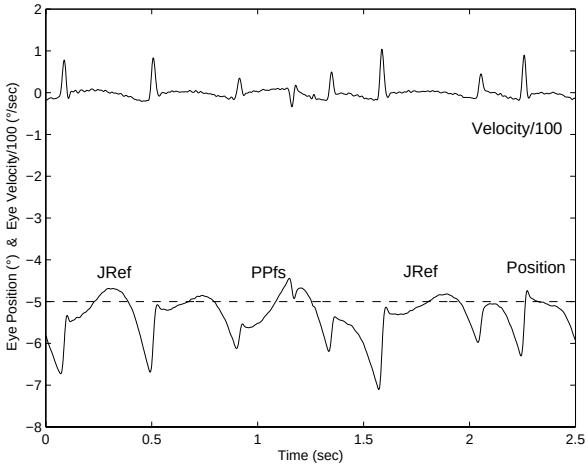

Figure 7. Human data that shows transition from a PPfs waveform to a jerk waveform at a gaze angle of -5°. Upper trace is velocity scaled down to 1/100 its original values to fit in the same graph as the position data (lower trace). JRef = Jerk Right with extended foveation.

Eye-movement data from individuals with jerk IN also show that with inattention, the foveating fast phase is delayed and the accelerating slow phase actually decelerates (i.e., there is a point of inflection) before the fast phase resets the fovea on target (Figure 8a). Thus, inattention reveals the underlying pendular nature of the oscillation. As soon as attention to the target is reestablished (either spontaneously or after verbal prompting by the experimenter), a foveating fast phase is executed and jerk waveforms return. Figure 8b shows a nice inattention section with large underlying pendular oscillations, which reverted to jerk waveforms after verbal prompting.

The conception of a resettable PMC+ is in accordance with the observations about inattention discussed above. The resetting of an oscillation (i.e., dumping energy) in a short amount of time is not a new concept in the ocular motor system. An eye-velocity storage mechanism has been postulated in the vestibulo-optokinetic system to account for the prolongation of vestibular nystagmus (VN) and the occurrence of optokinetic after-

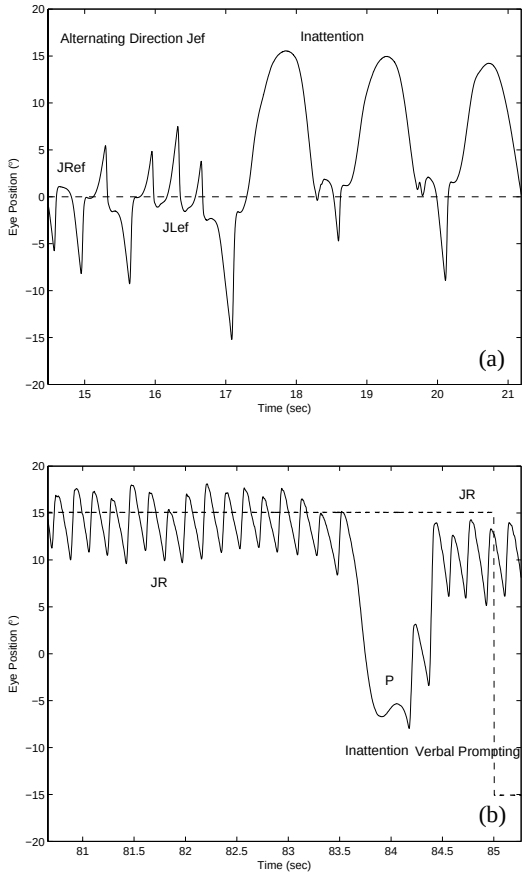

Figure 8. (a) Fixation in primary position with alternating direction jerk IN waveforms whose slow phases become pendular when inattention suppresses the fast phases. (b) Fixation at 15° right gaze with jerk right IN degenerating to pendular IN with inattention and returning to jerk after verbal prompting.

nystagmus (OKAN) [21]. Presentation of a subject-stationary full-field surround during VN and OKAN rapidly reduces activity related to eye velocity of the storage mechanism. This decrease in activity occurs with a shorter time constant compared to that in control trials, it has been called "dumping" [22]. The PMC+ resetting is also reasonable in engineering terms. A damping circuit needs to be discharged with all its energy storing devices in order to be reset correctly; this discharging takes time, which is consistent with the fact that our resetting signal from the foveating saccade motor command was 40 ms.

Simulations with various target inputs showed the robustness of this unified model. Compared to human data, the model outputs had less cycle-to-cycle variation. This was because this model was constructed under the assumption that this oscillating OMS is otherwise healthy, which is not always true in the case of a patient. Also, the abilities of gaze holding and generating accurate, consistent foveating saccades differ greatly in patients, which explains the large idiosyncratic differences in beat-to-beat accuracy even for patients with the same types of nystagmus waveforms.

Foveation-period quality is an important factor that contributes to visual acuity. The model relies on the fixation subsystem to prolong the time of low slip velocity. The fixation subsystem is a velocity-limiting system aimed at reducing retinal slip during foveation [23]. It follows foveating (including volitional) saccades; it is most effective when the target image falls within the fovea, and the slip velocity is relatively low. Depending on individual fixation capabilities, each individual's waveform shows different foveation quality. For example, in the jerk-right panels in Figure 6, the lower panel has "flatter" foveation than the upper one, indicating better potential visual acuity [24]. Tuning the fixation subsystem parameters in the OMS model could simulate waveforms with varying levels of fixation quality to match specific human data.

The step-input responses shown in Figure 5 exhibited the model's ability to produce waveforms with accelerating slow phases *towards* the null region (which, in this case, is assumed to be at primary position). This is a property found in eye movement data recordings of INS patients; our OMS model is the first model that successfully simulates this property.

The values of saccadic latency in the simulations are in agreement with human data. Preliminary data analysis on patients with PPfs, jerk, and dual jerk waveforms showed that nystagmus subjects had a higher latency than normal subjects for generating voluntary saccades. Average values for normal subjects are ~250 ms. Depending on which time of the cycle that the stimulus change occurred, the time needed to arrive at the target varied. This model took the normal subjects' average value of ~250 ms as the saccade latency. It can be altered to match values that reflect the performance of nystagmus subjects. Also, the time that the model needs to arrive at the target should be tested with stimuli occurring with different timing. Alterations to the model could be made if the model responses differed from human data.

The simulations of this robust behavioral OMS model demonstrate that both pendular and jerk waveforms can be generated by the same pursuit-system instability and support the hypothesis that most pendular and jerk INS waveforms are due to a loss of pursuit-system damping. Future work will simulate the seamless transitions between pendular, jerk-right, and jerk-left waveforms, regulated by Alexander's law. As we have seen in this paper, modeling OMS dysfunction (e.g., INS) continues to provide valuable insight into the functional structure of the OMS under both normal and pathological conditions.

5. ACKNOWLEDGEMENTS

This work was supported in part by the Office of Research and Development, Medical Research Service, Department of Veterans Affairs Merit Review (lfd).

6. REFERENCES

[1] CEMAS_Working_Group, "A National Eye Institute Sponsored Workshop and Publication on The Classification of Eye Movement Abnormalities and Strabismus (CEMAS). In The National Eye Institute Publications (www.nei.nih.gov)," National Institutes of Health, National Eye Institute, Bethesda, MD 2001.

[2] L.F. Dell'Osso and R.B. Daroff, "Congenital nystagmus waveforms and foveation strategy," **Doc Ophthalmol**, vol. 39, 1975, pp. 155-182.

[3] L.F. Dell'Osso, J.T. Flynn, and R.B. Daroff, "Hereditary congenital nystagmus: An intrafamilial study," **Arch Ophthalmol**, vol. 92, 1974, pp. 366-374.

[4] L.F. Dell'Osso and R.B. Daroff, "Eye movement characteristics and recording techniques," in **Neuro-Ophthalmology, 2nd Edition**, J.S. Glaser, Ed. Hagerstown: Harper and Row, 1990, pp. 279-297.

[5] L.F. Dell'Osso and R.B. Daroff, "Nystagmus and saccadic intrusions and oscillations," in **Duane's Clinical Ophthalmology, Vol. II, Chap. 11**, W. Tasman and E.A. Jaeger, Eds. Philadelphia: Lippincott-Raven, 1997, pp. 1-33.

[6] L.F. Dell'Osso and R.B. Daroff, "Clinical disorders of ocular movement," in **Models of Oculomotor Behavior and Control**, B.L. Zuber, Ed. West Palm Beach: CRC Press Inc, 1981, pp. 233-256.

[7] L.F. Dell'Osso, G. Gauthier, G. Liberman, and L. Stark, "Eye movement recordings as a diagnostic tool in a case of congenital nystagmus," **Am J Optom Arch Am Acad Optom**, vol. 49, 1972, pp. 3-13.

[8] L.F. Dell'Osso, "A Dual-Mode Model for the Normal Eye Tracking System and the System with Nystagmus. (Ph.D. Dissertation)," in *Electrical Engineering (Biomedical)*. Laramie: University of Wyoming, 1968, pp. 1-131.

[9] J.B. Jacobs, "An Ocular Motor System Model that Simulates Congenital Nystagmus, Including Braking and Foveating Saccades. (Ph.D. Dissertation)," in *Biomedical Engineering*. Cleveland: Case Western Reserve University, 2001, pp. 1-357.

[10] J.B. Jacobs and L.F. Dell'Osso, "Congenital nystagmus: hypothesis for its genesis and complex waveforms within a behavioral ocular motor system model," **JOV**, vol. 4, 2004, pp. 604-625.

[11] J.B. Jacobs and L.F. Dell'Osso, "A robust, normal ocular motor system model with latent/manifest latent nystagmus (LMLN) and dual-mode fast phases," in **Neurobiology of Eye Movements. From Molecules to Behavior—Ann NY Acad Sci 956**, vol. Ann NY Acad Sci 956, H.J. Kaminski and R.J. Leigh, Eds. New York: NYAS, 2002, pp. 604-607.

[12] L.F. Dell'Osso, R.W. Hertle, R.W. Williams, and J.B. Jacobs, "A new surgery for congenital nystagmus: effects of tenotomy on an achiasmatic canine and the role of extraocular proprioception," **J AAPOS**, vol. 3, 1999, pp. 166-182.

[13] R.W. Hertle, W. Anninger, D. Yang, R. Shatnawi, and V.M. Hill, "Effects of extraocular muscle surgery on 15 patients with oculo-cutaneous albinism (OCA) and infantile nystagmus syndrome (INS)," **Am J Ophthalmol**, vol. 138, 2004, pp. 978-987.

[14] R.W. Hertle, L.F. Dell'Osso, E.J. FitzGibbon, D. Thompson, D. Yang, and S.D. Mellow, "Horizontal rectus tenotomy in patients with congenital nystagmus. Results in 10 adults," **Ophthalmology**, vol. 110, 2003, pp. 2097-2105.

[15] D.A. Robinson, J.L. Gordon, and S.E. Gordon, "A model of smooth pursuit eye movements," **Biol Cyber**, vol. 55, 1986, pp. 43-57.

[16] L.A. Abel, L.F. Dell'Osso, and R.B. Daroff, "Analog model for gaze-evoked nystagmus," **IEEE Trans Biomed Engng**, vol. BME(25), 1978, pp. 71-75.

[17] L.A. Abel, L.F. Dell'Osso, D. Schmidt, and R.B. Daroff, "Myasthenia gravis: Analogue computer model," **Exp Neurol**, vol. 68, 1980, pp. 378-389.

[18] A.A. Kustov and D.L. Robinson, "Modified saccades evoked by stimulation of the Macaque superior colliculus account for properties of the resettable integrator," **J Neurophysiol**, vol. 73, 1995, pp. 1724-1728.

[19] L.F. Dell'Osso and R.B. Daroff, "Braking saccade--A new fast eye movement," **Aviat Space Environ Med**, vol. 47, 1976, pp. 435-437.

[20] J.B. Jacobs, L.F. Dell'Osso, and D.M. Erchul, "Generation of braking saccades in congenital nystagmus," **Neuro Ophthalmol**, vol. 21, 1999, pp. 83-95.

[21] T. Raphan, V. Matsuo, and B. Cohen, "Velocity storage in the vestibuloocular reflex arc (VOR)," **Exp Brain Res**, vol. 35, 1979, pp. 229-248.

[22] W. Waespe and U. Schwartz, "Characteristics of eye velocity storage during periods of suppression and reversal of eye velocity in monkeys," **Exp Brain Res**, vol. 65, 1986, pp. 49-58.

[23] J. Epelboim and E. Kowler, "Slow control with eccentric targets: evidence against a position-corrective model," **Vision Res**, vol. 33, 1993, pp. 361-380.

[24] L.F. Dell'Osso and J.B. Jacobs, "An expanded nystagmus acuity function: intra- and intersubject prediction of best-corrected visual acuity," **Doc Ophthalmol**, vol. 104, 2002, pp. 249-276.